Analysis on Raman gain coefficients in polarization maintaining photonic crystal fibers

Hong Fang (方 宏), Shuqin Lou (娄淑琴), Tieying Guo (郭铁英), and Shuisheng Jian (简水生)

Institute of Lightwave Technology, Beijing Jiaotong University, Beijing 100044

Received April 10, 2006

The Raman gain coefficients in polarization maintaining photonic crystal fibers (PM-PCFs) are analyzed in order to design fibers for linearly polarized Raman fiber laser with enhanced performances. The results show that a well designed germanium-doped PM-PCF can attain the value of Raman gain coefficient over 50 $W^{-1}\cdot km^{-1}$, going with very high birefringence and single mode operation at 1.55-μm signal wavelength and 1.45-μm pump wavelength.

OCIS codes: 060.0060, 060.2420, 140.3550.

Raman fiber lasers have found applications in telecommunications, medicine, and scientific areas, and most Raman fiber lasers reported to date have a randomly polarized output which is advantageous in such applications as distributed Raman amplification in telecommunications[1]. However, applications like harmonic generation, parametric conversion, and spectroscopy of gases require emission with a high degree of polarization. Moreover, the maximum Raman gain efficiency can be attained no other than the pump and signal have same polarization[2]. Therefore, some linearly polarized Raman generation in polarization maintaining birefringent fibers has been reported previously[2,3].

On the other hand, it has been already demonstrated that photonic crystal fibers (PCFs) greatly enhance nonlinear effects, and therefore, they represent an optimal solution as Raman amplification fibers[4], and a model that can be used to describe the Raman properties of PCFs accurately has been developed[5]. However, no analysis of Raman properties in polarization maintaining PCFs (PM-PCFs) has been presented so far. In this letter, we analyze how the Raman gain coefficients of PM-PCFs, where two of the air holes adjacent to the core are larger than the others, change with varying the structure parameters of PM-PCFs, and then the effect of germanium-doped core is also investigated.

The Raman gain coefficient $\gamma_{\rm R}$ is related to the frequency separation $\Delta\nu$ between the pump and Stokes, and is calculated according to[6]

$$\gamma_{\rm R}(\Delta\nu) = \iint_S C_{\rm SiSi}(\Delta\nu)(1-2m(x,y))i_{\rm s}(x,y)i_{\rm p}(x,y){\rm d}x{\rm d}y + \iint_S C_{\rm GeSi}(\Delta\nu)2m(x,y)i_{\rm s}(x,y)i_{\rm p}(x,y){\rm d}x{\rm d}y, \quad (1)$$

where S is the fiber cross section, it is important to mention that the contributions to the Raman gain coefficient are given only by the zones where the glass is present in, so the air holes are not included in the integral region; $m(x,y)$ is the germanium concentration; $C_{\rm SiSi}$ and $C_{\rm GeSi}$ are the Raman spectra relative to Si-O-Si and Ge-O-Si bridging bonds, respectively. In order to consider the peak Raman gain coefficient, we assume pump and signal wavelengths are 1.45 and 1.55 μm, respectively, so that $\Delta\nu = 13.2$ THz, and then, according to the prediction and experimental measurement reported in Ref. [6], $C_{\rm SiSi} = 33.4$ $\mu{\rm m}^2/({\rm W}\cdot{\rm km})$, $C_{\rm GeSi} = 118$ $\mu{\rm m}^2/({\rm W}\cdot{\rm km})$. $i_{\rm s}$, $i_{\rm p}$ are the normalized signal and pump intensities, respectively. They can be given by the definition of the Poynting vector as

$$i(x,y) = \frac{1}{P}{\rm Re}\left[\frac{\vec{E}\times\vec{H}^*}{2}\cdot\hat{z}\right] = \frac{1}{P}{\rm Re}\left[\frac{E_xH_y^* - E_y^*H_x}{2}\right], \quad (2)$$

where P is the integral of the intensity over the section of the fiber,

$$P = \iint_S {\rm Re}\left[\frac{\vec{E}\times\vec{H}^*}{2}\cdot\hat{z}\right]{\rm d}x{\rm d}y = \iint_S {\rm Re}\left[\frac{E_xH_y^* - E_y^*H_x}{2}\right]{\rm d}x{\rm d}y. \quad (3)$$

Because the fields extend along the entire transverse plane, the overall section of the PM-PCF, including the whole air holes, is the integral region here.

Then, the most important process is calculation of the magnetic field and the electric field. In this letter, a full-vector plane-wave method is used[7,8]. In order to test the accuracy of our calculation, we compare our predictions of the Raman gain coefficient to the results calculated through the finite element method (FEM) solver[5]. Consider a same triangular PCF as in Ref. [5], pitch $\Lambda = 4.2$ μm, relative hole diameter $d/\Lambda = 0.44$ and the diameter of the germanium-doped region $d_{\rm d} = 6$ μm. Figure 1 shows the relation between the values of $\gamma_{\rm R}$ at the frequency separation of 13.2 THz and germanium concentration in the doped core. The solid curve shows our results, and the open circles show the results reported in Ref. [5]. The agreement is excellent, showing that the calculation is accurate.

Figure 2 shows the schematic cross section of the PM-

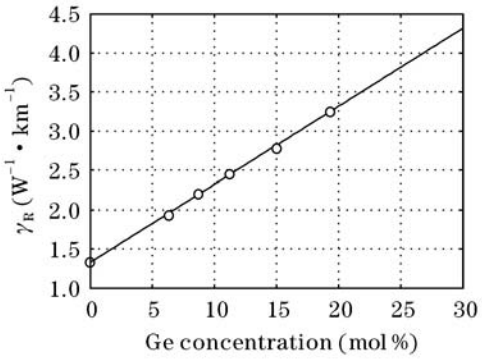

Fig. 1. Raman gain coefficients γ_R of triangular PCF as a function of germanium concentration in the doped core, the solid curve shows our results, and the open circles show the results reported in Ref. [5].

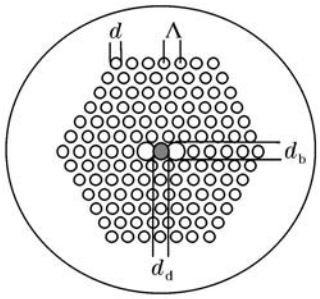

Fig. 2. Schematic cross section of PM-PCF.

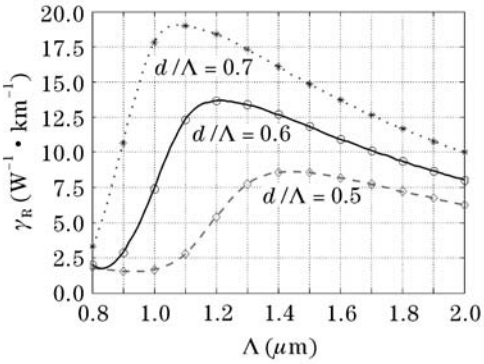

Fig. 3. Raman gain coefficients γ_R of PM-PCFs as a function of pitch Λ for various d/Λ.

PCF, having two large air holes with the diameter d_b adjacent to the core. In this letter we will analyze the Raman gain coefficient of this type of PM-PCF, which has much higher modal birefringence than the conventional polarization maintaining fibers[9].

Firstly, PM-PCFs with silica bulk have been considered. Figure 3 shows the Raman gain coefficients γ_R of PM-PCFs, with $d/\Lambda = 0.5$, 0.6, 0.7, and $d/d_b = 0.6$, as a function of Λ varying from 0.8 to 2. For a given value of d/Λ, there is an optimal value of Λ that maximizes γ_R, which is 1.4, 1.2, 1.1 μm for $d/\Lambda = 0.5$, 0.6, 0.7, respectively. In order to explain this phenomenon, let us consider two separate aspects: increasing the value of Λ will increase the effective area of mode A_{eff} or Raman effective area A_{eff}^R, so it results in reducing the value of γ_R. On the other hand, for a given wavelength, decreasing the value of Λ will weaken the confinement of the optical mode in the core, leading to reducing the value of γ_R also. Therefore, at a certain value of Λ between two extreme situations, γ_R becomes maximum. Moreover, the figure also shows that γ_R increases with the values of d/Λ, which can be explained that the greater filling fraction of air holes around the central silica core is, the higher field tightness is, leading to higher normalized intensities of optical mode.

Then, the Raman gain coefficients γ_R of PM-PCFs with various d/d_b are considered. Figure 4 shows γ_R of PM-PCFs, with $d/\Lambda = 0.5$, 0.6, 0.7, and $\Lambda = 1.4$, 1.2, 1.1 μm, respectively, which is the optimal values obtained by the previous study for various d/Λ, as a function of d/d_b. From the figure a very interesting phenomenon can be found, γ_R will be maximized when d/d_b is equal to a same value, 0.6, for these PM-PCFs. This rule is different from that for the birefringence, which becomes larger with the enhancing of size difference between these two kinds of holes all the while.

Afterwards, PM-PCFs with silica bulk and germanium-doped core were investigated. Figure 5 shows γ_R of the same three PM-PCFs as above, with fixing germanium concentration $m = 15$ mol%, as a function of the relative diameter of germanium-doped region d_d/Λ. It shows that there is an optimal value of $d_d/\Lambda = 1$—1.2 to maximize γ_R for each PM-PCF. From the result of simulation, it is confirmed to be wrong that the wider the doped region is the higher γ_R is, but when the doped region is nearly equal to the effective core of PM-PCF, the maximum of γ_R will be attained. The reason is that when the

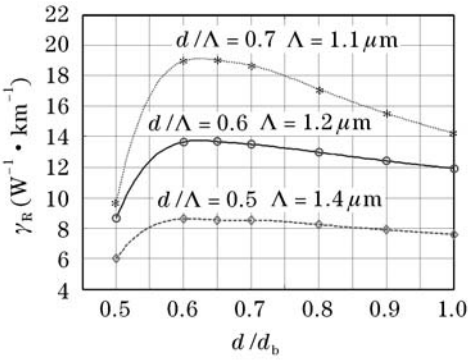

Fig. 4. Raman gain coefficients γ_R of PM-PCFs, with $d/\Lambda = 0.5$, 0.6, 0.7, and $\Lambda = 1.4$, 1.2, 1.1 μm, respectively, as a function of d/d_b.

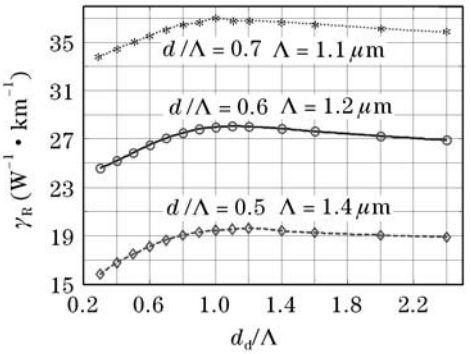

Fig. 5. Raman gain coefficients γ_R of PM-PCFs, with $d/\Lambda = 0.5$, 0.6, 0.7, $\Lambda = 1.4$, 1.2, 1.1 μm, respectively and $m = 15$ mol%, as a function of d_d/Λ.

doped region is smaller than the effective core, widening it will bring forth two kinds of improvements for γ_R. One is increasing the refractive index difference between the effective core and effective cladding, which results in higher field tightness. The other is that the more mode field lies in the doped region, the greater γ_R is by reason of $C_{GeSi} > C_{SiSi}$. However, when the doped region is larger than the effective core, widening it will bring forth slightly impairing for γ_R, because the field tails will be able to leak out through the bridges between the air holes due to the same material.

Table 1 shows the parameters of the PM-PCFs that optimize Raman performances and relevant maximum of γ_R. These values of γ_R are much higher than the well designed Raman fibers with conventional structure which can reach values of γ_R near to 5—6 $W^{-1}\cdot km^{-1}$.

An investigation was carried out on the germanium concentration in the doped core. Figure 6 shows γ_R of the three PM-PCFs, with fixing structure parameters as Table 1, as a function of the germanium concentration which has been progressively incremented starting from 5 mol% up to 30 mol% with a step of 5 mol%. As the germanium concentration increases, the values of γ_R increase linearly. Galeener *et al.*[10] have measured that the peak relative Raman cross-section of germanium is 9.2 times greater than that of silica, and then, Davey *et al.*[11] reported that Raman gain coefficient for the SiO_2-GeO_2 glass is in excellent agreement with a linear interpolation between the values for SiO_2 and GeO_2.

Therefore

$$\gamma_R^{SiO_2-GeO_2} = \gamma_R^{SiO_2} + m \times \gamma_R^{SiO_2} \times (9.2-1)/100\%, \quad (4)$$

where $\gamma_R^{SiO_2-GeO_2}$ is the Raman gain coefficient of the fibers with germanium-doped core, and $\gamma_R^{SiO_2}$ is the Raman gain coefficient of the pure silica fibers without germanium. As an example, we can estimate from Fig. 6 that the solid curve has the slope of 111 $W^{-1}\cdot km^{-1}\cdot mol^{-1}$. And as seen from Fig. 4, $\gamma_R^{SiO_2}$ = 13.6 $W^{-1}\cdot km^{-1}$ for this PM-PCF, so the slope predicted by Eq. (4) should be $13.6 \times (9.2-1)/100\% = 111.52$ $W^{-1}\cdot km^{-1}\cdot mol^{-1}$, which is inagreement with that estimated from Fig. 6. So, it is also confirmed that our method is an accurate tool to predict the Raman gain coefficients of PM-PCFs.

Table 1. Parameters of the PM-PCFs that Optimize Raman Performances and the Relevant Maximum γ_R, with Germanium Concentration Equal to 15 mol%

d/Λ	Λ (μm)	d/d_b	d_d/Λ	γ_R ($W^{-1}\cdot km^{-1}$)
0.5	1.4	0.6	1.2	19.6443
0.6	1.2	0.6	1.1	28.0252
0.7	1.1	0.6	1.0	36.9753

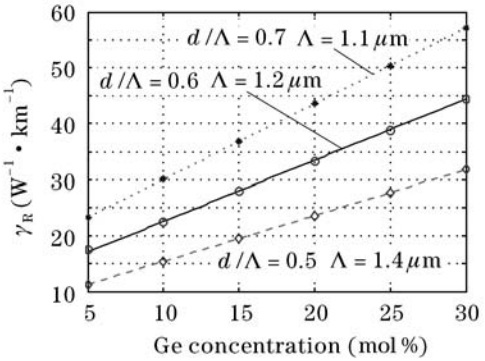

Fig. 6. Raman gain coefficients γ_R of PM-PCFs, with d/Λ = 0.5, 0.6, 0.7, and Λ = 1.4, 1.2, 1.1 μm, respectively, as a function of germanium concentration.

High values of γ_R are indeed what we expect, but not the all we must consider. The birefringence and single mode characteristic affected by increasing of germanium concentration are also needed to watch out. Figure 7 shows the birefringence and 3rd mode cutoff wavelength of these PM-PCFs as a function of germanium concentration. The values of birefringence at wavelength of 1.45 μm are little smaller than the ones at 1.55 μm, it is because that the mode field diameter becomes smaller as the wavelength is shortened, and this results in a reduction in modal asymmetry. In addition, there is very little increment with the enhancement of germanium concentration, and the lowest birefringence of these PM-PCFs is near to 4×10^{-3} at 1.55 and 1.45 μm, which is much larger than that of a conventional panda fiber.

Since the 1st and 2nd modes are the two linearly polarization modes of fundamental mode, the cutoff wavelength of 3rd mode is considered for the condition of single mode operation. When the wavelength is longer than the cutoff wavelength of 3rd mode, any mode except fundamental mode will be cut off. As Fig. 7 shows, the cutoff wavelength of 3rd mode moves to the long wavelength with the enhancement of germanium concentration, the reason is that the refractive index difference between core and cladding increases with increasing of germanium concentration, i.e. numerical aperture increases, thus the wavelength needs to be enhanced to ensure single mode operation. Figure 7 also shows that even though the germanium concentration is up to 30 mol%, 3rd mode cutoff wavelengths of these PM-PCFs are lower than 1.2 μm, it is to say that the transmission of signal at 1.55 μm and pump at 1.45 μm are both single mode operation. This characteristic cannot be achieved in the conventional fibers.

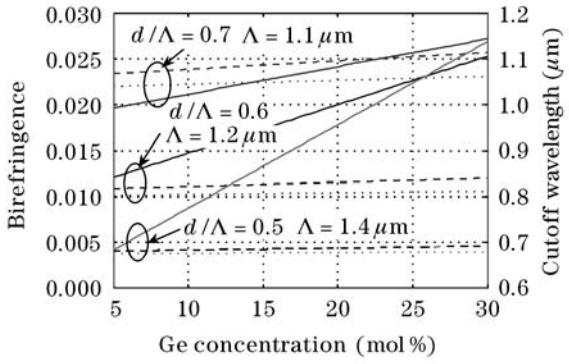

Fig. 7. Birefringence and 3rd mode cutoff wavelength of PM-PCFs, with d/Λ = 0.5, 0.6, 0.7, and Λ = 1.4, 1.2, 1.1 μm, respectively, as a function of germanium concentration. The solid lines scaled by right y-axis show 3rd mode cutoff wavelength, the dashed and dotted lines scaled by left y-axis show birefringence for wavelengths of 1.55 and 1.45 μm, respectively.

In conclusion, the Raman properties in PM-PCFs, including that structure parameter of PM-PCFs, germanium-doped region and germanium concentration have been analyzed. These properties have effect on the Raman gain coefficient γ_R. It is shown that a well designed germanium-doped PM-PCF can attain the value of Raman gain coefficient over 50 $W^{-1}\cdot km^{-1}$, going with very high birefringence and single mode operation at signal wavelength of 1.55 μm and pump wavelength of 1.45 μm, which cannot be achieved in conventional fibers. These properties of PM-PCFs are very valuable for the new type of linearly polarized Raman fiber laser.

This work was supported by the National "863" Program of China (No. 2004AA31G200) and the Foundation of Beijing Jiaotong University. H. Fang's e-mail address is macrofang@263.net or macrofang@tom.com.

References

1. J. Zhang, V. Dominic, M. Misey, S. Sanders, and D. Mehuys, in *Proceedings of Conf Optical Amplifiers and Their Applications* OMB4 (2000).
2. R. H. Stolen, IEEE J. Quantum Electron. **15,** 1157 (1979).
3. S. A. Skubchenko, M. Y. Vyatkin, and D. V. Gapontsev, IEEE Photon. Technol. Lett. **16,** 1014 (2004).
4. Z. Yusoff, J. H. Lee, W. Belardi, T. M. Monro, P. C. Teh, and D. J. Richardson, Opt. Lett. **27,** 424 (2002).
5. M. Bottacini, F. Poli, A. Cucinotta, and S. Selleri, J. Lightwave Technol. **22,** 1707 (2004).
6. J. Bromage, K. Rottwitt, and M. E. Lines, IEEE Photon. Technol. Lett. **4,** 24 (2002).
7. S. G. Johnson and J. D. Joannopoulos, Opt. Express **8,** 173 (2001).
8. S. Guo and S. Albi, Opt. Express **11,** 167 (2003).
9. K. Suzuki, H. Kubota, and S. Kawanishi, Opt. Express **9,** 676 (2001).
10. F. L. Galeener, J. C. Mikkelsen, R. H. Geils, W. J. Mosby, M. Tanaka, and M. Fujita, Appl. Phys. Lett. **32,** 34 (1978).
11. S. T. Davey, D. L. Williams, B. J. Ainslie, B. J. M. Rothwell, and B. Wakefield, IEE Proceedings-Optoelectronics **136,** 301 (1989).